and

$$\frac{Ae^{j\beta_1 L}}{Be^{-j\beta_1 L}} = e^{j\phi}.$$

It can be easily shown that, if there is to be a nontrivial solution for amplitudes A and B, ϕ and L must be related by the equation

$$e^{j\beta_1 L} - e^{2j\phi - j\beta_1 L} = 0$$

which has the solution

$$\beta_1 L = \phi. \tag{26}$$

The required spacing between the partitions to resonate the TE_{011} mode can be found by solving (26) for L, using the values of ϕ given in Figs. 4(a) and 4(b). The spacing for the TE_{01n} resonant mode can be found by simply adding $(n-1)2\pi$ to ϕ before solving for L.

The numerical results for the TE_{011} mode are shown in Figs. 6(a), 6(b), and (7) in the form of curves of L/b against $k_0 b$ for typical values of the parameter b/a. The range of resonant frequencies over which the cavity can be tuned by varying L/b is a strong function of b/a. The value $b/a = 1.831$ gives the maximum tuning range.

The numerical results shown in Fig. 7 are for $b/a = 2.082$. This value is commonly used in practice since it corresponds to locating the cylindrical partition at the radius where the electric field of the TE_{01} mode has its maximum intensity, i.e., $J_1(\Gamma_1 r)$ has a maximum at $r = b/2.082$. This value of b/a was used in the design of the cavity shown in Fig. 1. The data point in Fig. 7 corresponding to the measured values of L/b and $k_0 b$ for this cavity indicates that the theoretical and experimental results are in good agreement.

References

[1] M. Sucher and J. Fox, *Handbook of Microwave Measurements*, 3rd ed., vol. 2. New York: Interscience, 1963, ch. 9.

[2] A. W. Adey, "Microwave refractometer cavity design," *Canad. J. Tech.*, vol. 34, pp. 519–521, March 1957.

[3] M. C. Thompson, Jr., F. E. Freethey, and D. M. Waters, "End plate modifications of X-band TE_{011} cavity resonators," *IRE Trans. on Microwave Theory and Techniques (Correspondence)*, vol. MTT-7, pp. 388–389, July 1959.

[4] D. C. Thorn and A. W. Straiton, "Design of open-ended microwave resonant cavities," *ibid.*, pp. 389–390.

[5] R. O. Gilmer and D. C. Thorn, "Some design criteria for open-ended microwave cavities," University of New Mexico, Albuquerque, N. Mex., Tech. Rept. EE-65, June 1962.

[6] S. Ramo and J. R. Whinnery, *Fields and Waves in Modern Radio*, 2nd ed. New York: Wiley, 1953, pp. 364–366, 374–379.

[7] R. E. Collin, *Fieid Theory of Guided Waves*. New York: McGraw-Hill, 1960, ch. 10.

[8] R. Mittra and C. P. Bates, "An alternative approach to the solution of a class of Wiener-Hopf and related problems," University of Illinois, Urbana, Ill., Antenna Lab. Rept. 65-21, February 1966.

[9] B. Noble, *Methods Based on the Wiener-Hopf Technique for the Solution of Partial Differential Equations*. New York: Pergamon, 1958.

[10] A. E. Heins and S. Silver, "The edge conditions and field representation theorems in the theory of electromagnetic diffraction," *Proc. Cam. Phil. Soc.*, vol. 51, pp. 149–161, January 1955.

[11] For an example of this technique see P. M. Morse and H. Feshbach, *Methods of Theoretical Physics*, vol. 1. New York: McGraw-Hill, 1953, pp. 382–385.

Theory of Direct-Coupled-Cavity Filters

RALPH LEVY, SENIOR MEMBER, IEEE

Abstract—**A new theory is presented for the design of direct-coupled-cavity filters in transmission line or waveguide. It is shown that for a specified range of parameters the insertion-loss characteristic of these filters in the case of Chebyshev equal-ripple characteristic is given very accurately by the formula**

$$\frac{P_0}{P_L} = 1 + h^2 T_n^2 \left[\frac{\omega_0}{\omega} \frac{\sin\left(\pi \frac{\omega}{\omega_0}\right)}{\sin \theta_0'} \right]$$

where h defines the ripple level, T_n is the first-kind Chebyshev polynomial of degree n, ω/ω_0 is normalized frequency, and θ_0' is an angle proportional to the bandwidth of a distributed lowpass prototype filter. The element values of the direct-coupled filter are related directly to the step impedances of the prototype whose values have been tabulated. The theory gives close agreement with computed data over a range of parameters as specified by a very simple formula. The design technique is convenient for practical applications.

Manuscript received November 8, 1966; revised January 27, 1967. The work reported in this paper was supported by a Ministry of Aviation research contract.

The author is with the Department of Electrical and Electronic Engineering, University of Leeds, Yorkshire, England.

Introduction

A NEW TREATMENT of the classic problem of direct-coupled microwave filter design is presented. These filters consist of TEM transmission line or waveguide cavities coupled either by series capacitances or by shunt inductances, as shown in Figs. 1(a) and 1(b), respectively. It will be assumed that the waveguide or transmission line is of uniform impedance. The more general case is perhaps of less importance for economic reasons, but it has been discussed by Young [1], and the theory presented here may be extended as described by that author.

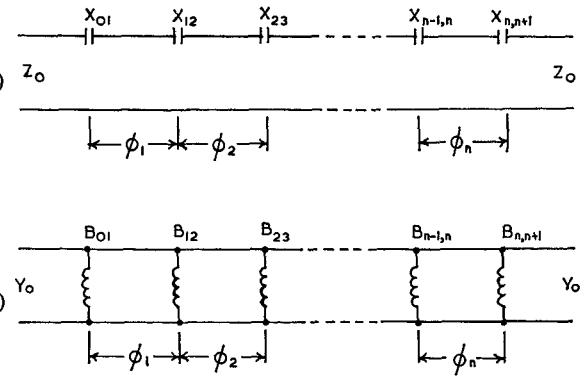

Fig. 1. Direct-coupled filter, (a) with series capacitance couplings, and (b) with shunt inductance couplings.

In this paper frequency will be specified in normalized form as ω/ω_0, the ratio of the frequency to the synchronous, resonant, or design center frequency. In the case of waveguide filters the normalized frequency must be replaced everywhere by normalized reciprocal guide wavelength, i.e., the quantity $\lambda g_0/\lambda g$.

In common with all previous theories it is assumed that the coupling reactances or susceptances behave as perfect lumped circuit elements. In practice this is not quite the case, but it would be very difficult to take the actual frequency variation of microwave obstacles into account. Any deviations from the idealized model are thought to be small, probably less than the errors inherent in the theory, which is approximate. This point is justified in a later section.

An exact theory for the idealized model would require further development of multivariable function theory, which so far as its application to network problems is concerned is in its infancy [2].

There are two methods of microwave direct-coupled filter design in general use. The older method of Cohn [3] is based on a lowpass prototype, and gives good results for bandwidths up to approximately 20 percent if, in the case of Chebyshev response, the ripple VSWR V is not too close to unity. The two conditions under which Cohn's theory leads to accurate designs have been given by Young [1] as follows:

a) For filter bandwidths ≤ 20 percent,

$$V > 1 + (2w)^2 \tag{1}$$

where V is the specified ripple VSWR and w is the fractional bandwidth, and

b)
$$R \gg \left(\frac{1}{w}\right)^n \tag{2}$$

where R is the product of the junction VSWR's of the associated quarter-wave prototype filter [1]. The results obtained by Whiting [4] for seven cavity filters, where (2) always holds, indicate that (1) may be rather overly optimistic in some cases; e.g., for $V = 1.05$ Whiting showed that Cohn's theory gives good results only to a bandwidth certainly less than 5 percent, whereas (1) suggests that it should hold to 10 percent.

The second well-established design theory is that of Young [1], and is based on the quarter-wave transformer or distributed lowpass prototype circuit. In this method a suitable prototype is chosen, and the filter designed by equating the synchronous (design) frequency VSWR of each reactive coupling discontinuity of the filter to that of the corresponding junction VSWR of the prototype filter. The spacings between the reactances are adjusted to give synchronous performance. This statement is equivalent mathematically to Cohn's original formulas [3], as given here in (21). The frequency variation of the reactive couplings modify the known response of the quarter-wave transformer prototype. The actual response may be estimated utilizing a number of graphs giving a bandwidth contraction factor and also the movements of the upper and lower cutoff frequencies of the filter. In addition, the attenuation in the stopbands of the filter may be predicted with good accuracy. Although it is thus possible to predict the performance of a filter based on a given distributed prototype, it is not posssible to carry out the reverse operation without using a trial-and-error procedure.

In summary it may be said that Cohn's method gives simple formulas for filter design, but gives poor results for filters with low VSWR ripple tolerance and moderate bandwidths [(1) and (2)], while Young's method gives excellent results for low VSWR ripple tolerances and large bandwidth specifications, but is not nearly as simple to use as Cohn's.

The present paper presents a method which tends to combine the desirable features of the previous techniques, i.e., it combines the accuracy of Young's method with the simplicity of Cohn's, and leads to filter designs which are quite accurate for all but the most extreme specifications. The design is based on the quarter-wave transformer or distributed lowpass prototype filter [5], [6] but all the essential features (bandwidth, cutoff frequencies, stopband attenuation) are predicted using a single formula.

Theory

Consider the shunt-inductive-coupled filter of Fig. 1(b). This must be treated using the concept of the impedance inverter [3]. The lowpass prototype filter is shown diagrammatically in Fig. 2(a), and in exactly equivalent form using impedance inverters [1], [3] in Fig. 2(b). Here the transmission lines of electrical length θ', which take the value π at the band center frequency of the first harmonic, as shown in Fig. 3, must be regarded as series-type resonators, whereas the admittance inverter form of this prototype filter has shunt resonators [7]. The exact Pi equivalent circuit of a transmission line [3] is given in Fig. 4, where the shunt elements of the Pi network are very small compared with the series element. The $1:-1$ ideal transformer represents the phase reversal of a half-wave line, and since it plays no part in the filter performance it may be neglected.

In order to draw an equivalence between the prototype circuit and the reactance-coupled filters of Fig. 1, it is necessary to find a suitable low- to bandpass mapping function which takes into account the frequency variation of the reactive couplings.

Consider the shunt-inductive-coupled filter of Fig. 1(a). This is redrawn in Fig. 5(a) as a set of impedance inverters of the type shown in Fig. 5(b), each separated by lines of electrical length θ. The impedance inverter of Fig. 5(b) consists of a shunt inductance jX at the center of a short length of transmission line of electrical length $-\phi$, and was a concept first introduced by Cohn [3]. Now the transfer matrix of an ideal impedance inverter is given by

$$\begin{bmatrix} 0 & \pm jK \\ \pm j/K & 0 \end{bmatrix} \tag{3}$$

while the transfer matrix of the actual impedance inverter of Fig. 5(b) is

$$\begin{bmatrix} A & B \\ C & A \end{bmatrix} = \begin{bmatrix} \cos\phi - \dfrac{\sin\phi}{2X/Z_0} & -j\left(\sin\phi + \dfrac{\cos\phi - 1}{2X/Z_0}\right)Z_0 \\ -\dfrac{j}{Z_0}\left(\sin\phi + \dfrac{\cos\phi + 1)}{2X/Z_0}\right) & \cos\phi - \dfrac{\sin\phi}{2X/Z_0} \end{bmatrix}. \tag{4}$$

Hence the condition for this to represent an impedance inverter is that $A=0$, i.e.,

$$\phi = \tan^{-1}\frac{2X}{Z_0}. \tag{5}$$

The matrix (4) then becomes the same as that of matrix (3) (with the + sign), where

$$K = Z_0 \tan\frac{\phi}{2} \tag{6}$$

$$\frac{X}{Z_0} = \frac{K/Z_0}{1 - (K/Z_0)^2}. \tag{7}$$

The above theory ignores the frequency variation of the shunt inductances, and in practice the K of (6) must be a function of frequency. Since ϕ is small even for fairly broadband filters, $(K/Z_0)^2 \ll 1$, and (7) gives

$$\frac{X}{Z_0} \simeq \frac{K}{Z_0} \tag{8}$$

i.e., K and X have approximately the same frequency dependence, namely, directly proportional to frequency. In order to take this frequency dependence into account it is necessary to replace K by $K(\omega/\omega_0)$, where ω_0 is the design or synchronous frequency, so that matrix (4) is represented very well by the matrix

$$\begin{bmatrix} 0 & jK\dfrac{\omega}{\omega_0} \\ j/K\dfrac{\omega}{\omega_0} & 0 \end{bmatrix} = \begin{bmatrix} 0 & jmK \\ j/mK & 0 \end{bmatrix} \tag{9}$$

where

$$m = \frac{\omega}{\omega_0}. \tag{10}$$

In order to obtain an impedance inverter which is truly frequency-invariant, it is necessary to split matrix (9) into three parts:

$$\begin{bmatrix} 0 & jmK \\ \dfrac{1}{mK} & 0 \end{bmatrix} = \begin{bmatrix} \sqrt{m} & 0 \\ 0 & \dfrac{1}{\sqrt{m}} \end{bmatrix}\begin{bmatrix} 0 & jK \\ \dfrac{j}{K} & 0 \end{bmatrix}\begin{bmatrix} \dfrac{1}{\sqrt{m}} & 0 \\ 0 & \sqrt{m} \end{bmatrix}. \tag{11}$$

The first and third component matrices of the RHS of (11) represent ideal transformers with a frequency-dependent turns ratio, and the central matrix represents the desired ideal impedance inverter. The equivalent circuit of the matrix (11) is shown in Fig. 6. The impedance inverter is given by the shunt inductance X_0 at the center of the line $-\phi_0$, where ϕ_0 is given in terms of X_0 by (5), X_0 being the value of X at the synchronous frequency. The next step is to replace each approximate impedance inverter in Fig. 5(a) by its more exact representation in Fig. 6, from which a typical portion of the filter appears in the form shown in Fig. 7.

It is now obvious that in order to draw an equivalence between this form of the filter and the prototype of Fig. 2(b) it is necessary only to find the equivalence between the basic line length θ' of the prototype and the line length θ of Fig. 7 *bounded by ideal transformers with frequency-dependent turns ratio*. The transfer matrix of any of the latter circuits as shown boxed within the dotted lines of Fig. 7 is given by

$$\begin{bmatrix} \dfrac{1}{\sqrt{m}} & 0 \\ 0 & \sqrt{m} \end{bmatrix}\begin{bmatrix} \cos\theta & jZ_0\sin\theta \\ \dfrac{j}{Z_0}\sin\theta & \cos\theta \end{bmatrix}\begin{bmatrix} \sqrt{m} & 0 \\ 0 & \dfrac{1}{\sqrt{m}} \end{bmatrix} = \begin{bmatrix} \cos\theta & j\dfrac{Z_0}{m}\sin\theta \\ \dfrac{j}{Z_0}m\sin\theta & \cos\theta \end{bmatrix} \tag{12}$$

whereas the transfer matrix of the basic prototype line length is

$$\begin{bmatrix} \cos\theta' & jZ_0\sin\theta' \\ \dfrac{j}{Z_0}\sin\theta' & \cos\theta' \end{bmatrix}. \tag{13}$$

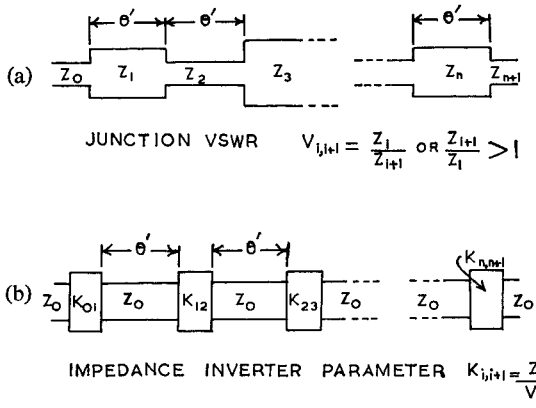

Fig. 2. (a) Lowpass prototype filter, (b) using impedance inverters.

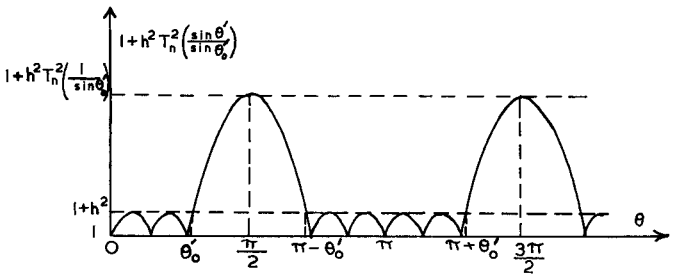

Fig. 3. Typical characteristic of a Chebyshev equal-ripple distributed lowpass prototype filter showing the first harmonic passband.

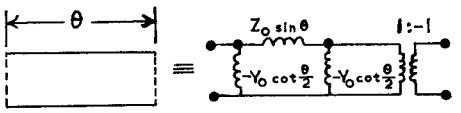

Fig. 4. Exact equivalent circuit of a transmission line.

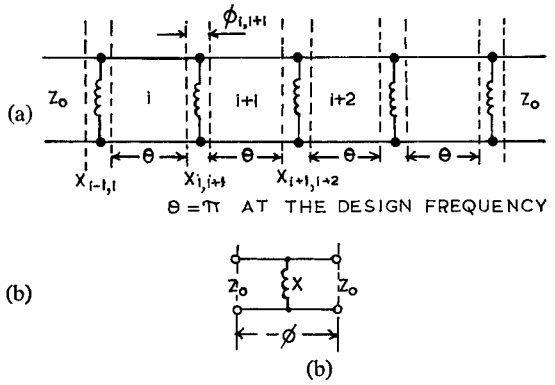

Fig. 5. (a) Section of a shunt-inductive-coupled bandpass filter. (b) An impedance inverter.

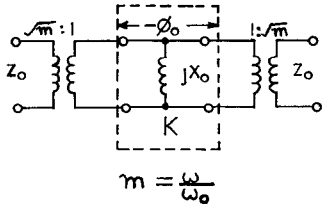

Fig. 6. More exact equivalent circuit of the impedance inverter shown in Fig. 5(b).

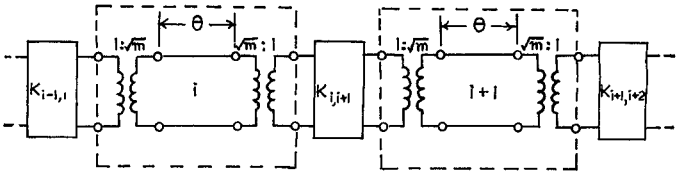

Fig. 7. Equivalent circuit of a typical central portion of a reactive-coupled filter showing true impedance inverters, and cavities associated with ideal transformers having frequency-dependent turns ratio.

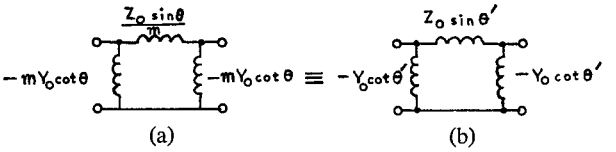

Fig. 8. Equivalence to be established between (a) the circuit representing a cavity of a reactance-coupled filter and (b) the circuit representing a cavity of the impedance-inverter-coupled prototype.

The transfer matrices (12) and (13) must be regarded as those of series resonators of the type shown in Fig. (4), not only because we are working on the basis of impedance inverters which require series-type resonators, but also because the small shunt admittances of the Pi network are swamped by the large adjacent admittances in the shunt-reactance-coupled filter. The series-capacitance-coupled filter is a dual circuit treated by the admittance inverter concept, and leads to identical results. Hence the equivalence to be established is shown in Fig. 8. Near the design frequency the shunt arms of the Pi networks may be neglected, and the equivalence is established by the equation

$$\sin\theta' = \frac{\sin\theta}{m} = \frac{\sin(\pi\omega/\omega_0)}{\omega/\omega_0}. \tag{14}$$

This is the required equation relating the reactance-coupled filter to the prototype; it will be shown to give remarkably good results, considering its simplicity. If the prototype filter has Chebyshev characteristics given by the following insertion-loss function [5], [6] (defined as the ratio of available power P_0 from the generator to the power P_L delivered to the load),

$$\frac{P_0}{P_L} = 1 + h^2 T_n^2\left(\frac{\sin\theta'}{\sin\theta_0'}\right), \tag{15}$$

then the insertion-loss function of the reactance-coupled filter is given by

$$\frac{P_0}{P_L} = 1 + h^2 T_n^2\left[\frac{\omega_0}{\omega}\,\frac{\sin\frac{\pi\omega}{\omega_0}}{\sin\theta_0'}\right]. \tag{16}$$

The bandedge frequencies ω_1 and ω_2 are given by

$$\frac{\omega_0}{\omega_1}\sin\pi\frac{\omega_1}{\omega_0} = -\frac{\omega_0}{\omega_2}\sin\pi\frac{\omega_2}{\omega_0} = \sin\theta_0'. \tag{17}$$

Design Procedure

The design procedure is now fully established. Given the normalized bandedge frequencies of the filter ω_1/ω_0 and ω_2/ω_0, (17) is solved for θ_0'. The solution is shown graphically in Fig. 9. In an actual specification ω_1 and ω_2 will be given, but in this case ω_0 is readily found from Fig. 9 by finding the value of θ_0' with the required $(\omega_2/\omega_0)/(\omega_1/\omega_0)$ ratio. The passband ripple level is given in terms of the parameter h of (16) either as

$$10 \log_{10} (1 + h^2) \qquad \text{(dB)}$$

or as a VSWR related to h by the equation

$$h = \frac{V - 1}{2\sqrt{V}} \cdot \tag{18}$$

A value of n, the number of cavities in the filter, will be decided by the stopband attenuation specification, and may be found readily by application of (16).

The value of θ_0' is related to the fractional bandwidth of the equivalent prototype quarter-wave transformer, the parameter required by the published tables [5], [6] by the equation

$$w_q \text{ (or } BW) = \frac{4\theta_0'}{\pi} \cdot \tag{19}$$

Hence the three parameters necessary to specify the prototype filter—namely, n, w_q, and ripple VSWR—have been established, and the step impedances or junction VSWR's of this prototype are then either found from the tables [5], [6] or determined by a suitable approximation [as in (27)].[1] The reactance values of the reactance-coupled filter are determined from the prototype junction VSWR's as described by Young [1], namely, by equating these to the VSWR's of corresponding reactance couplings of the actual filter, leading to the equation (refer to Fig. 1)

$$\frac{Z_0}{X_{i,i+1}} = \frac{Y_0}{B_{i,i+1}} = \sqrt{V_{i,i+1}} - \frac{1}{\sqrt{V_{i,i+1}}} \cdot \tag{20}$$

The electrical lengths ϕ_i of the cavities are given by the well-known formulas [1], [3]

$$\begin{aligned} \tan \phi_i &= \pi - \frac{1}{2}\left[\tan^{-1}\frac{2X_{i-1,i}}{Z_0} + \tan^{-1}\frac{2X_{i,i+1}}{Z_0}\right] \\ &= \pi - \frac{1}{2}\left[\tan^{-1}\frac{2B_{i-1,i}}{Y_0} + \tan^{-1}\frac{2B_{i,i+1}}{Y_0}\right] \end{aligned} \tag{21}$$

where $i = 1, 2, \cdots n$.

[1] It is worth recording a correction to (22) of reference [6], which should read

$$Z_r = Z_{n-r+1} \ (n \text{ odd}); \qquad Z_r = S/Z_{n-r+1} \ (n \text{ even}).$$

A further error occurs in Table 8 where results in BW columns 0.20 to 0.70 for VSWR values 1.01 and 1.02 should be interchanged.

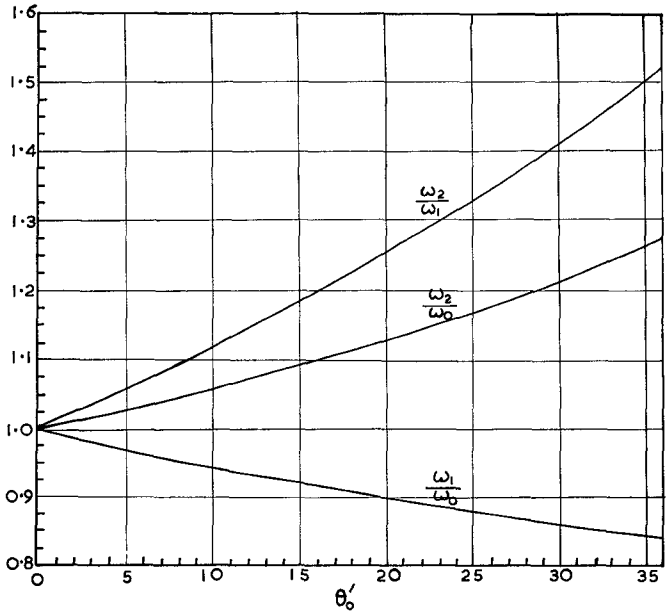

Fig. 9. Solution of (17).

Comparison with Theories of Cohn and Young

Cohn's results [3] may be obtained by approximating $\sin [\pi(\omega/\omega_0)]$ around $\omega = \omega_0$ by $\pi[(\omega/\omega_0) - 1]$. The angle θ_0' is given by (19). Since the fractional bandwidth w of a narrowband filter is related to w_q by a factor 2, we have

$$\theta_0' = \frac{\pi w}{2} = \pi \frac{(\omega_2 - \omega_1)}{(\omega_2 + \omega_1)} \cdot \tag{22}$$

With the further approximation (justified for narrowband filters) $\sin \theta_0' \simeq \theta_0'$, (17) reduces to

$$\pi \frac{\omega_0}{\omega_1}\left(1 - \frac{\omega_1}{\omega_0}\right) = -\pi \frac{\omega_0}{\omega_2}\left(1 - \frac{\omega_2}{\omega_1}\right) = \pi \frac{(\omega_2 - \omega_1)}{(\omega_2 + \omega_1)}$$

leading to the equation (Fig. 10 in Cohn [3])

$$\omega_0 = \frac{2\omega_1\omega_2}{\omega_1 + \omega_2} \cdot \tag{23}$$

Cohn's low- to bandpass transformation is obtained from (16), and is given by carrying out the above approximation to the equation

$$\frac{\omega'}{\omega_1'} = \frac{\omega_0}{\omega} \frac{\sin \dfrac{\pi\omega}{\omega_0}}{\sin \theta_0'}$$

which, using (23), reduces to

$$\frac{\omega'}{\omega_1'} \simeq \frac{2\left(\dfrac{1}{\omega} - \dfrac{1}{\omega_0}\right)}{\left(\dfrac{1}{\omega_1} - \dfrac{1}{\omega_2}\right)} \cdot \tag{24}$$

This is (4) in Cohn [3] with guide wavelength replaced by reciprocal of frequency, as required.

Cohn's expressions for the coupling reactances are obtained by using the formulas for the junction VSWR's in the limiting case of a narrowband distributed lowpass prototype filter as given by Young [1], i.e.,

$$\left.\begin{aligned} V_{01} &= V_{n,n+1} = \frac{2}{\pi}\frac{g_1\omega_1'}{w} = \frac{g_1}{C} \\ V_{i,i+1} &= \frac{4}{\pi^2}\frac{\omega_1'^2}{w^2}g_{i+1}g_i = \frac{g_{i+1}g_i}{C^2} \end{aligned}\right\} \tag{25}$$

for $i=i, 2, \cdots, (n-1)$, where

$$C = \frac{\pi}{\omega_1'}\frac{\omega_2-\omega_1}{\omega_2+\omega_1}. \tag{26}$$

Here the g_i are the normalized elements of the *lumped-element* lowpass prototype filter [2]. The coupling reactances are given by (20), i.e.,

$$\left.\begin{aligned} \frac{Z_0}{X_{01}} = \frac{Y_0}{B_{01}} &= \sqrt{\frac{g_1}{C}} - \sqrt{\frac{C}{g_1}} \\ \frac{Z_0}{X_{i,i+1}} = \frac{Y_0}{B_{i,i+1}} &= \sqrt{\frac{g_ig_{i+1}}{C}} - \sqrt{\frac{C}{g_ig_{i+1}}} \\ \text{for } i &= 1, 2, \cdots, (n-1) \\ \frac{Z_0}{X_{n,n+1}} = \frac{Y_0}{B_{n,n+1}} &= \sqrt{\frac{g_n}{C_0r}} - \sqrt{\frac{C_0r}{g_n}}, \end{aligned}\right\} \tag{27}$$

where r is the terminating resistance of the prototype filter. Equations (26) and (27) are given in Figs. 5 and 10 in Cohn [3], completing the derivation of all his formulas. These are seen to be limiting forms of the new formulas in the case of narrowband filters after approximating sin $(\pi\omega/\omega_0)$ by $\pi[(\omega/\omega_0)-1]$. One result of this approximation is that the theory fails to predict the harmonic passbands of the reactance-coupled filter.

Young's Theory

Young [1] bases his theory on the distributed lowpass prototype but needs to guess a value of θ_0' to obtain a trial prototype. He presents graphs of bandwidth contraction factor and movement of band center frequency to predict the "distortion" caused by the frequency variation of the coupling reactances, which in the new theory is given automatically by (16). The information on bandwidth contraction factor was obtained by analyzing a number of filter designs by digital computer. If the design specification is not met by the first prototype, a modified prototype is chosen, and the above process repeated. The theory will give good results to bandwidths so large that the bandpass filter becomes a highpass filter for all practical purposes.

The theory presented in the present paper is limited to filters up to approximately 40-percent bandwidth, which will cover all normal requirements. Discussions follow on the method adopted to test the theory, the errors involved, and the theory's range of applicability.

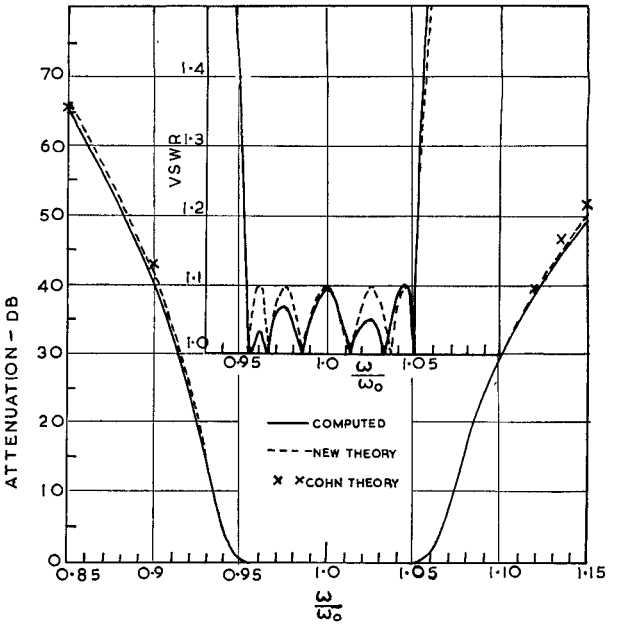

Fig. 10. Theoretical and computed results of a filter expected to give good agreement (Example 1 of text).

Limitations on the Value of Experimental as Compared with Computed Results

For several reasons it would be rather difficult to establish the validity of a microwave filter theory by measurements on actual filters. One must be quite sure that the obstacle susceptances actually have the assumed values; it is difficult and expensive to achieve the very close tolerances which must be held, and a large number of such filters would be required to check the theory over a wide range of the various parameters. Thus in order to test the validity of the theory, the practice of previous authors has been adopted [1], [3] and the theoretical predictions compared with the response of idealized model filters found by computation on a high-speed digital computer. Experience has shown that actual filters give performances in very close agreement with the computed results. The only practical case published which appears to show a marked deviation [4] is open to some doubt since in that case the inductive susceptances were designed by use of an approximate theoretical formula rather than by direct measurement.

The computer technique is open to the objection that actual filters differ from the idealized model in that the obstacle susceptances are not exactly proportional to ω (for capacitive gap filters) or to λ_g (for waveguide filters). It can be shown, however, that the deviation of a practical filter from the idealized model is quite small, and is in a direction which tends to *improve* the agreement between practice and theory. Take, for example, the case of direct-coupled inductive-iris waveguide filters. Inspection of graphic data [8] shows that the deviation of the shunt susceptance values from their idealized values over a 30-percent guide-wavelength band is approximately 1 percent at the edges of this band. Since this error not only is small but also has the same sign for

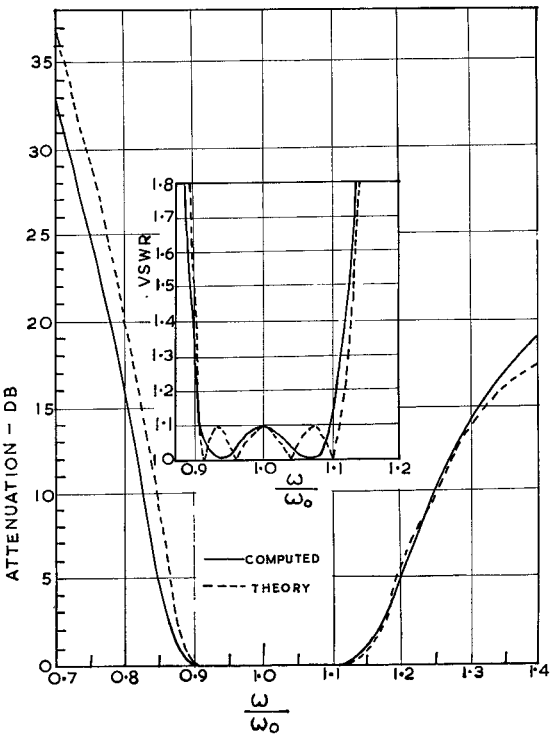

Fig. 11. Theoretical and computed results of a filter designated as a borderline case (Example 2 of text).

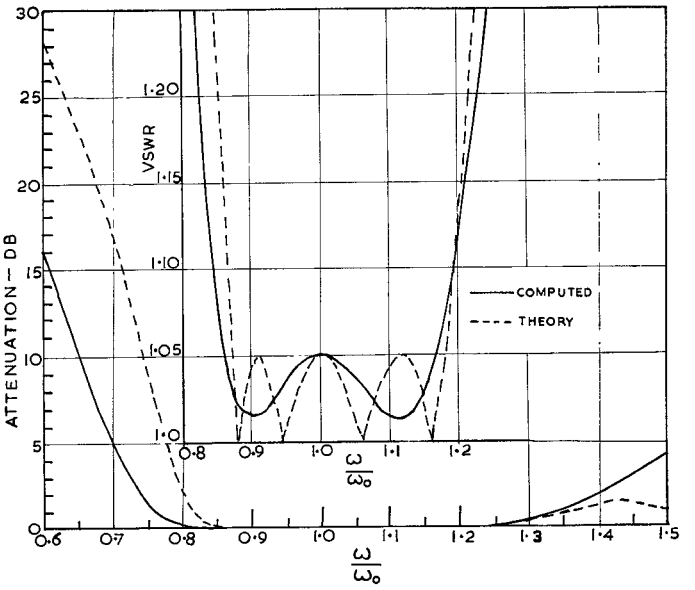

Fig. 12. Theoretical and computed results of a filter whose specification lies outside the range of validity of the theory (Example 3 of text).

all the obstacles in the filter, it could not be expected to cause any significant error in the ripple level, but only in the cutoff frequencies. The effect of deviation from lumped susceptance behavior is to introduce an additional frequency transformation which distorts the frequency axis slightly. For inductive irises in waveguide, the susceptances are slightly larger than their idealized values at frequencies below the midband frequency, and slightly smaller above the midband frequency. Hence the lower frequency cutoff is moved upward in frequency, and the higher frequency cutoff is also moved upward in frequency. The overall bandwidth of the filter tends to remain as predicted by the idealized model. The attenuation on the low-frequency side of the filter is increased, and on the high-frequency side it is decreased. Inspection of the results discussed in the following section and presented in Figs. 10, 11, and 12 reveals that this tendency would, fortuitously, give better agreement between the theory and the computed results. The case depicted in Fig. 12 illustrates the effect most clearly. The practical filter would be expected to have cutoff frequencies approximately 1 percent higher than those predicted by the idealized model, which would bring the practical performance into closer agreement with the theory.

It would be interesting to carry out a more detailed investigation of the computed performance of the idealized model filters compared with *computed* practical cases where the actual variation of obstacle susceptance with frequency [8] would be taken into the computer program.

Limitations of the New Theory

Thus in order to test the validity of the theory, a very large number of filters were designed for $n=2$ to $n=12$ elements having fractional bandwidths ranging from 10 to 43 percent and VSWR ripple levels from 1.01 to 1.50. The computed response of each filter was then compared with the theoretical response given by (16). It is found that except in extreme cases, as specified below, the bandedge frequencies and stopband attenuation are in excellent agreement with the theory. Young [1] had established that the passband ripple levels are reproduced quite accurately, and this was confirmed except for very low VSWR levels (1.01 or 1.02) for moderate or large bandwidth filters, where the small errors in the theory tend to produce a slightly higher ripple level in practice. As a criterion by which to establish the theory's range of applicability it was decided to classify as acceptable only those designs within about ± 10-percent deviation from the theoretical both for bandwidth and for attenuation level (in dB) far into the stopbands. Most filters give results well inside these limits, but Table I indicates the limiting cases. The interpretation of Table I is that for a given number of cavities and a given bandwidth, the ripple VSWR must be greater than the designated value. It has been established that all the information given in Table I may be summarized by a very simple rule, namely, that the criterion requires the value of R (the product of the prototype junction VSWR's [1], [5]) or of L (the maximum stopband attenuation level of the prototype as given in the tables of reference [6]) to be greater than a value given by

$$L = 10 \log_{10} \frac{(R+1)^2}{4R} = \begin{cases} 6n \text{ dB for } n = 2 \\ 7n \text{ dB for } n = 3 \\ 8n \text{ dB for } n \geq 4. \end{cases} \quad (28)$$

TABLE I

MINIMUM PASSBAND VSWR RIPPLE LEVELS FOR FILTERS GIVING AGREEMENT WITH THEORY TO WITHIN APPROXIMATELY ±10-PERCENT DEVIATION IN BANDWIDTH AND IN STOPBAND ATTENUATION LEVEL IN dB. [SEE ALSO (28).]

w_a or BW	0.2	0.3	0.4	0.5	0.6	0.7	0.8
θ_0'	9	13.5	18	22.5	27	31.5	36
Bandwidth (%)	10.03	15.10	20.23	25.49	30.93	36.70	43.12
No. of Cavities (n)							
2	1.10		1.50				
3			1.20				
4	1.05		1.10		1.50		
5	1.01	1.02	1.10	1.20			
6		1.01	1.02		1.20		
7			1.01		1.10	1.50	1.50
8				1.05			
9							
10					1.05		
11							
12						1.05	

Some examples of the results given by the theory will now be presented. Most specifications for direct-coupled filters are for narrow or moderate bandwidths, i.e., 10 percent or less, and for these cases the agreement between the theoretical formula (16) and the computed results is almost perfect. Therefore, only one example of such a filter will be given, the remaining examples indicating the limitations of the theory in extreme cases.

EXAMPLES

1) Bandwidth 10 Percent, Six Cavities, Chebyshev Ripple VSWR 1.10

This design is one considered by previous authors [1], [3] and each obtained satisfactory results. Here, in order to avoid interpolation from tabulated data, the bandedges are chosen to be at values $\omega_1/\omega_0 = 0.9524$, $\omega_2/\omega_0 = 1.0527$, which corresponds to a value of θ_0' of exactly 9°. The comparison between computed values and theory is given in Fig. 10, which also indicates points computed by Cohn's formula. It will be seen that the theory predicts the location of the bandedges exactly, although the passband response is slightly distorted from the correct equal-ripple behavior. The maximum deviation from theory of the attenuation in the stopband is less than 1 dB to an attenuation level of at least 66 dB on the low-frequency side and to at least 50 dB on the high-frequency side.

2) Bandwidth 20 Percent, Four Cavities, Chebyshev Ripple VSWR 1.10

This example, which is designated as a limiting case in Table I, was also used as an illustration by Young [1]. Here the theoretical design based on $\theta_0' = 18°$ gives $\omega_1/\omega_0 = 0.9093$, $\omega_2/\omega_0 = 1.1116$, i.e., a bandwidth of 20.23 percent. The theoretical and computed values are shown in Fig. 11. The computed results show the bandedges as 0.909 and 1.103, giving an actual bandwidth of 19.4 percent. Young's theory [1] based on the same prototype predicts the bandedges at 0.902 and 1.110, i.e., a bandwidth of 20.8 percent, which is slightly less accurate than the present theory in this instance.

3) Bandwidth 30 Percent, Four Cavities, Chebyshev Ripple 1.05

This specification lies well outside the limits of applicability as designated in Table I or by (28), and would not be expected to give good results. A very similar example was taken by Young [1], the difference being that the VSWR specification was chosen as 1.07. The comparison between theory and computed values in Fig. 12 shows that the present theory predicts the position of the bandedges remarkably closely, i.e., 0.860 compared with the theoretical 0.8707 at the low-frequency edge, and 1.165 compared with 1.180 at the high-frequency edge. The bandwidth is almost correct. The most serious deviation from theory occurs in the prediction of the stopband attenuation at low frequencies. In this respect, however, the theory gives more accurate results than formula (13) of Young [1] which predicts an even higher attenuation at low frequencies and negative attenuation at high frequencies (e.g., −6 dB at $\omega/\omega_0 = 1.5$).

CONCLUSIONS

A new design theory for direct-coupled microwave filters has been shown to give good agreement with computed response characteristics. Basically the theory is derived by combining and extending previous work done by Cohn [3] and Young [1]. It has been shown that the essential characteristics of direct-coupled filters may be predicted accurately by a single insertion-loss formula (16). The values of the coupling reactances are derived from published tables of distributed lowpass prototype filters [5], [6], or in narrowband cases which may not be tabulated by use of approximate but very accurate formulas (25). A simple relationship (28) specifies the range of design parameters (number of cavities, bandwidth, ripple VSWR) for which the insertion-loss formula (16) may be expected to give good results for prediction of the bandedge frequencies and for the stopband attenuation.

Since it is based on a single insertion-loss formula and on tabulated or easily derivable prototype filter parameters, the design technique is very suitable for practical applications.

References

[1] L. Young, "Direct-coupled cavity filters for wide and narrow bandwidths," *IEEE Trans. on Microwave Theory and Techniques*, vol. MTT-11, pp. 162–178, May 1963.

[2] J. O. Scanlan, "Progress in linear circuit theory 1963–1966," *Progress in Radio Science*, to be published. (Paper presented at the URSI General Assembly, Munich, Germany, 1966.)

[3] S. B. Cohn, "Direct-coupled-resonator filters," *Proc. IRE*, vol. 45, pp. 187–196, February 1957.

[4] K. Whiting, "The effect of increased design bandwidth upon direct-coupled-resonator filters," *IEEE Trans. on Microwave Theory and Techniques (Correspondence)*, vol. MTT-11, pp. 557–560, November 1963.

[5] L. Young, "Tables for cascaded homogeneous quarter-wave transformers," *IRE Trans. on Microwave Theory and Techniques*, vol. MTT-7, pp. 233–237, April 1959; and "Correction to 'Tables for cascaded homogeneous quarter-wave transformers'," vol. MTT-8, pp. 243–244, March 1960.

[6] R. Levy, "Tables of element values for the distributed low-pass prototype filter," *IEEE Trans. on Microwave Theory and Techniques*, vol. MTT-13, pp. 514–536, September 1965.

[7] G. L. Matthaei, L. Young, and E. M. T. Jones, *Microwave Filters, Impedance-Matching Networks, and Coupling Structures*. New York: McGraw-Hill, 1964, pp. 144–149 and 427–438.

[8] N. Marcuvitz, *Waveguide Handbook*. New York: McGraw-Hill, 1951.

A Frequency Transformation for Commensurate Transmission-Line Networks

EDWARD G. CRISTAL, SENIOR MEMBER, IEEE

Abstract—**The frequency transformation $W=1/S$, where $S=\tanh(\gamma L)$, is investigated for commensurate transmission-line networks consisting of stubs, resistors, ideal transformers, and unit elements. This transformation takes transmission-line transformers into transmission-line lowpass filters and vice versa, lowpass (or bandstop) filters into highpass (or bandpass) filters and vice versa, and elliptic-function bandstop filters into elliptic-function bandpass filters and vice versa. The practicality of the transformation lies in the fact that element values of the transformed network are easily related to the corresponding element values of the original network. The transformation is useful because it provides an alternative viewpoint for synthesis, and because it reduces the number of tables of designs needed for various filter types. Several examples of designs using the transformation are given. One design is an unusual narrowband 3-dB directional coupler.**

I. Introduction

FREQUENCY transformations are commonly used in lumped-element network theory to convert a given filter network into a related filter network. For example, an often used frequency transformation is [1], [2]

$$s' \rightarrow As, \tag{1}$$

where the symbol $\rightarrow$ stands for "is replaced by," A is a constant, the primed variable is that of the original network, and the unprimed variable is that of the transformed network.[1] Transformation (1) is used to scale the bandwidth of the existing network to another preferred value. Other commonly used frequency transformations in lumped filter theory are [1], [2]

$$s' \rightarrow A/s \qquad \text{(lowpass to highpass transformation)} \tag{2}$$

$$s' \rightarrow w\left(\frac{s}{\omega_0}\right) + \left(\frac{\omega_0}{s}\right) \qquad \text{(lowpass to bandpass transformation)} \tag{3}$$

$$s' \rightarrow \frac{1}{w\left(\frac{s}{\omega_0}\right) + \left(\frac{\omega_0}{s}\right)} \qquad \text{(lowpass to bandstop transformation).} \tag{4}$$

It is emphasized that in all cases the usefulness of these transformations lies in the fact that their effects on the responses of the network are *easily* related to changes in the element values of the network. Because such frequency transformations are available, a given lowpass filter may function as a prototype for a number of different types of filters, obviating the compilation of a multitude of designs for lowpass, highpass, bandpass, and bandstop filters.

Analogous transformations would be equally useful for commensurate transmission-line networks, if they could be developed. For the special class of commensurate transmission-line networks consisting of open- and short-circuited stubs, ideal transformers, and resistors, but without unit elements [18] (i.e., quarter-wavelength lines), transformations (1) through (4) can indeed be used. In most cases, however, realization of commensurate transmission-line networks without unit elements is impractical or impossible. Unfortunately, in the more general case of commensurate transmission-line networks, consisting of open- and short-circuited stubs, ideal transformers, resistors, and unit ele-

Manuscript received September 21, 1966; revised December 22, 1966. The work reported in this paper was supported by the U. S. Army Electronics Command Laboratories, Fort Monmouth, N. J., under Contract DA-28-043-AMC-02266(E).

The author is with the Stanford Research Institute, Menlo Park, Calif.

[1] Throughout this paper we shall use primed variables to represent parameters of the original network and unprimed variables for those in the tranformed network.